PAPER

Enhancing the understanding of fragmentation processes in hadrontherapy and radioprotection in space with the FOOT experiment

To cite this article: S Colombi *et al* 2021 *Phys. Scr.* **96** 114013

View the article online for updates and enhancements.

Physica Scripta

PAPER

Enhancing the understanding of fragmentation processes in hadrontherapy and radioprotection in space with the FOOT experiment

S Colombi[1] , A Alexandrov[2,3,4,5], B Alpat[6], G Ambrosi[6], S Argir[7,8], R Arteche Diaz[9], N Bartosik[7], G Battistoni[10], N Belcari[11,12], E Bellinzona[13], S Biondi[1,14], M G Bisogni[11,12], G Bruni[1], P Carra[11,12], P Cerello[7], E Ciarrocchi[11,12], A Clozza[15], A Del Guerra[11,12], M De Simoni[16,17], A Di Crescenzo[2,3], B Di Ruzza[13], M Donetti[7], Y Dong[10,18], M Durante[19,20], R Faccini[16,17], V Ferrero[7], E Fiandri[6,21], C Finck[22], E Fiorina[7], M Fischetti[16,23], M Francesconi[11,12], M Franchini[1,14], G Franciosini[16,17], G Galati[2], L Galli[12], V Gentile[2,24], G Giraudo[7], R Hetzel[25], E Iarocci[15], M Ionica[6], A Iuliano[3], K Kanxheri[6], A C Kraan[12], V Lante[26], C La Tessa[13,27], M Laurenza[15], A Lauria[2,3], E Lopez Torres[7,9], M Marafini[16,28], C Massimi[14], I Mattei[10], A Mengarelli[1], A Moggi[12], M C Montesi[2,3], M C Morone[29,30], M Morrocchi[11,12], S Muraro[10], F Murtas[17], A Pastore[31], N Pastrone[7], V Patera[16,23], F Pennazio[7], P Placidi[6,32], M Pullia[26], F Raffaelli[12], L Ramello[7,33], R Ridolfi[1,14], V Rosso[11,12], C Sanelli[15], A Sarti[16,23], G Sartorelli[1,14], O Sato[34], S Savazzi[26], L Scavarda[7,8], A Schiavi[16,23], C Schuy[19], E Scifoni[13], A Sciubba[15,23], A Sécher[22], M Selvi[1], L Servoli[6], G Silvestre[6,21], M Sitta[7,33], R Spighi[1], E Spiriti[15], G Sportelli[11,12], A Stahl[25], V Tioukov[2], S Tommasini[15], F Tommasino[13,27], M Toppi[15,23], G Traini[16,17], S M Valle[10], M Vanstalle[22], M Villa[1,14], U Weber[19], R Zarrella[1,14] and A Zoccoli[1,14]

1 Istituto Nazionale di Fisica Nucleare (INFN), Section of Bologna, Bologna, Italy
2 Istituto Nazionale di Fisica Nucleare (INFN), Section of Napoli, Napoli, Italy
3 University of Napoli, Department of Physics "E. Pancini", Napoli, Italy
4 National University of Science and Technology, MISIS, RUS-119049 Moscow, Russia
5 Lebedev Physical Institute of the Russian Academy of Sciences, RUS-119991 Moscow, Russia
6 Istituto Nazionale di Fisica Nucleare (INFN), Section of Perugia, Perugia, Italy
7 Istituto Nazionale di Fisica Nucleare (INFN), Section of Torino, Torino, Italy
8 University of Torino, Department of Physics, Torino, Italy
9 CEADEN, Centro de Aplicaciones Tecnologicas y Desarrollo Nuclear, Havana, Cuba
10 Istituto Nazionale di Fisica Nucleare (INFN), Section of Milano, Milano, Italy
11 Istituto Nazionale di Fisica Nucleare (INFN), Section of Pisa, Pisa, Italy
12 University of Pisa, Department of Physics, Pisa, Italy
13 Trento Institute for Fundamental Physics and Applications, Istituto Nazionale di Fisica Nucleare (TIFPA-INFN), Trento, Italy
14 University of Bologna, Department of Physics and Astronomy, Bologna, Italy
15 Istituto Nazionale di Fisica Nucleare (INFN), Laboratori Nazionali di Frascati, Frascati, Italy
16 Istituto Nazionale di Fisica Nucleare (INFN), Section of Roma 1, Rome, Italy
17 University of Rome La Sapienza, Department of Physics, Rome, Italy
18 University of Milano, Department of Physics, Milano, Italy
19 Biophysics Department, GSI Helmholtzzentrum für Schwerionenforschung, Darmstadt, Germany
20 Technische Universität Darmstadt Institut für Festkörperphysik, Darmstadt, Germany
21 University of Perugia, Department of Physics and Geology, Perugia, Italy
22 Université de Strasbourg, CNRS, IPHC UMR 7871, F-67000 Strasbourg, France
23 University of Rome La Sapienza, Department of Scienze di Base e Applicate per l'Ingegneria (SBAI), Rome, Italy
24 Gran Sasso Science Institute, L'Aquila, Italy
25 RWTH Aachen University, Physics Institute III B, Aachen, Germany
26 Centro Nazionale di Adroterapia Oncologica (CNAO), Pavia, Italy
27 University of Trento, Department of Physics, Trento, Italy
28 Museo Storico della Fisica e Centro Studi e Ricerche Enrico Fermi, Rome, Italy
29 University of Rome Tor Vergata, Department of Physics, Rome, Italy
30 Istituto Nazionale di Fisica Nucleare (INFN), Section of Roma Tor Vergata, Rome, Italy
31 Istituto Nazionale di Fisica Nucleare (INFN), Section of Bari, Bari, Italy
32 University of Perugia, Department of Engineering, Perugia, Italy
33 University of Piemonte Orientale, Department of Science and Technological Innovation, Alessandria, Italy
34 Nagoya University, Department of Physics, Nagoya, Japan

E-mail: colombi@bo.infn.it

Abstract

During proton and carbon ions cancer treatment, nuclear interactions of the beam nuclei with the patient tissues always occur: the former leads to target fragmentation only, the latter to both projectile and target fragments production. In proton therapy the low-energy, high-charge and therefore short-range fragments produced along the beam path in the target fragmentation process may have higher biological effectiveness compared to protons, resulting in a not negligible effect on the delivered dose in a region before the tumor site. In carbon treatments the long range of projectile fragments results in a dose deposition in the healthy tissues behind the tumor site. Therefore, precise fragmentation cross section data would be of great importance to further optimize treatments. At the same time, such data would help improving the design of the shielding of spaceships, especially in view of long distance travels (i.e. Mars human exploration). In fact, nuclear fragmentation occurring between the space background radiation and spacecrafts materials changes the composition of the radiation field and thus the dose received by the astronauts. The FOOT (FragmentatiOn Of Target) experiment has been designed to investigate nuclear fragmentation processes of interest for particle therapy and space radiation protection with a precision in the cross section measurements around 5%. In this work the physics motivations of FOOT and the final design of the experiment will be presented. A performances study of the electronic setup based on FLUKA Monte Carlo simulations and a preliminary analysis of experimental data are reported as well.

1. Introduction

Today, the application of charged particle beams in cancer therapy is a well-established strategy and its combination with surgery and chemotherapy is becoming an increasingly reliable approach for the treatment of deep-seated solid tumors [1]. Currently, protons and ^{12}C ions are used in clinical practice, due to their characteristic depth-dose deposition profile featuring a pronounced peak (the Bragg Peak—in the following referred as BP) at the end of the range. By changing the kinetic energy of the incident ions, the position of the peak can be precisely shifted to the desired depth in tissue in order to deposit the majority of energy in correspondence of the tumor sparing the healthy tissues surrounding it. Clinical energies typically span between 60 and 250MeV for protons and up to 400 MeV/u for ^{12}C ions, in order to cover a 15–35 cm range in water and deliver treatments to various disease sites.

Nuclear interactions between the primary beam and the patient's body occur during treatment [2], leading to the production of both beam and target fragmentation. Primary beam ions can fragmentate in lower atomic number particles emitted along the beam path with energy close to the one of the primary beam, thus penetrating more deeply and leading to a dose deposition tail beyond the BP [2]. Instead, the fragmentation of the target nuclei produces low-energy and therefore short-range (order of 10–$100\,\mu$m) fragments isotropically emitted in the target frame. Both the produced projectile and target fragments could affect the Relative Biological Effectiveness (RBE, i.e. biological effectiveness of charged particles compared to therapeutic photons) of the primary beam, thus contributing to biological damage.

In carbon ions treatments an increased RBE value in correspondence of the BP region (i.e. the tumor region) due to the increasing beam Linear Energy Transfer (LET) [3] emerges. Such effect is related to the beam fragmentation, which modifies the delivered dose distribution to the patient's body. However, measurements dedicated to the characterization of projectile fragments for several energy-target combinations of interest for particle therapy are still incomplete and strongly required. Specifically, the beam of interest for particle therapy applications are the species either currently available in particle therapy or considered promising alternatives, such as ^{12}C, ^{16}O and ^{4}He at energies between 200 MeV/u and 400 MeV/u, while the reference targets are ^{16}O, ^{12}C and ^{1}H nuclei, being the most abundant elements in the human tissues [4, 5]. In proton treatments a fixed RBE equal to 1.1 [6] over the whole range is currently adopted in clinical practice, however the experiments show a significant increase in RBE above 1.1 [7]. It has been recently suggested [8] that target fragmentation could be responsible of this RBE increasing. Although, target fragmentation process has been almost completely neglected so far because of the experimentally difficulties in detecting target fragments due to their short range. Therefore, cross sections data for the production of both heavy and light target fragments produced in the interaction of proton beams up to 200MeV with ^{16}O and ^{12}C target are of great importance to understand the impact of nuclear interaction on proton RBE.
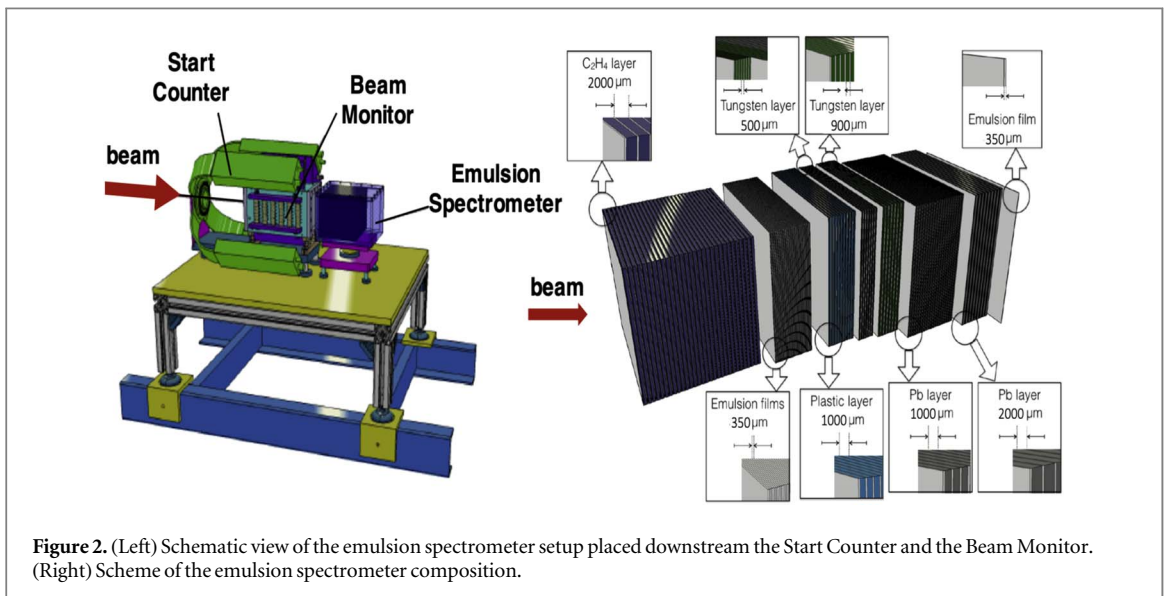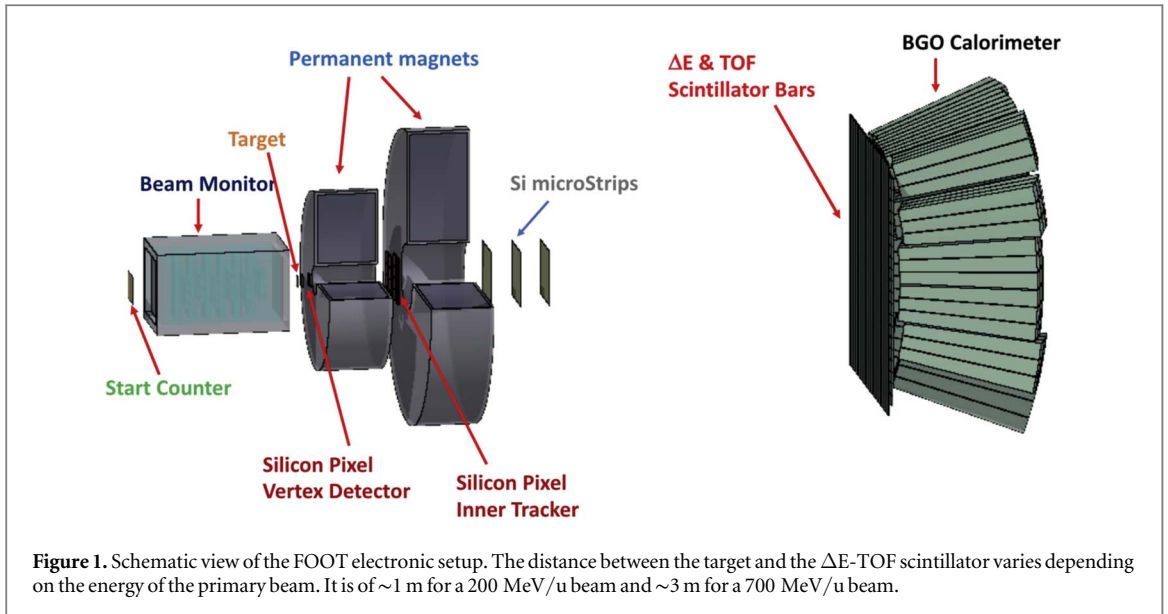
The same fragmentation mechanisms play a fundamental role also in space radioprotection. In fact, the radiation environment in space can lead to serious health risks for astronauts, especially in long duration and far from Earth space missions (like human explorations to Mars foreseen in the next deep decade). At present, the

only effective countermeasure is passive shielding, which can modify the spectrum of radiation traversing the spacecraft wall due to nuclear fragmentation processes occurring. The three main sources of energetic particles in space are the following: Solar Particle Events (SPEs), mainly composed by protons emitted from the Sun during coronal mass ejections and solar flares with an energy reaching few GeV; Galactic Cosmic Rays (GCRs), composed by protons (∼86%), helium (∼12%) and heavier ions (∼1%), with a broad energy distribution (from 10 MeV/u to the TeV/u region) peaked in the range 100–800 MeV/n [9]; geomagnetically trapped particles, composed of protons up to few hundreds MeV and electrons up to 100keV confined in the Van Allen belts by the Earth magnetic field. GCRs and SPEs are the most critical hazard for humans during deep space exploration outside the magnetosphere of our planet. In fact, they can interact with the spaceship hull producing lighter and highly penetrating radiation able to inflict a lethal dose and affect the stability of electronic devices [9]. Due to the inverse proportion between the mass stopping power and the atomic weight of the target, light materials rich in hydrogen are more effective for shielding purposes. Polyethylene (C_2H_4) is the best compromise so far. Experimental data investigating the fragments production for beam-target combinations relevant in space radiation applications will be of great help to select innovative shielding materials and provide recommendations on space radioprotection for different mission scenarios. Specifically, as primary beam should be considered the most abundant particle species in space (i.e. proton, ^{4}He, ^{7}Li, ^{12}C, ^{16}O) in the energy range up to 1000 MeV/u as proxy for the GCRs and SPEs [10] , while as target polyethylene and aluminum represent the most widely employed materials for spaceship shielding.

The FragmentatiOn Of Target (FOOT) project [11] is an applied nuclear physics experiment aiming to perform fragmentation studies of relevance for particle therapy and radioprotection in space. The FOOT experiment has been designed to measure with ∼5% accuracy fragmentation double differential cross sections with respect to the kinetic energy and the generation angle of the emitted fragments [12, 13]. The FOOT measurements campaign includes beams of ^{4}He, ^{12}C, ^{16}O in the energy range spanning between 200MeV/u and 700 MeV/u impinging on thin C, C_2H_4 and Al targets. The experimental data collected by the FOOT experiment would be of great importance for benchmarking Monte Carlo (MC) codes, which are extensively used by the scientific communities both in the hadrontherapy and space radioprotection fields. In fact, the available transport codes suffer from many uncertainties and they need to be verified with reliable experimental data.

2. The FOOT experiment

The FOOT experiment has been approved and funded by the Italian National Institute for Nuclear Physics (INFN) in 2017. The project will provide useful and still missing experimental data for the characterization of both projectile and target fragments in the energy range of particle therapy (40 to 400 MeV/u) and space radiation (700 to 1000 MeV/u). The detection of target fragments is particularly challenging because of the very short range travelled, resulting in a low probability to escape also the thinnest target practically feasible and in an excessively long beam time required to collect a sufficient amount of data. The maximum acquisition rate of the experiment (i.e. 1 kHz) makes pointless any attempt to gather a good statistic by increasing the beam intensity. Thus, target fragmentation induced by 50–250 MeV proton beams will be studied taking advantage of an inverse kinematic approach. Specifically, ^{12}C, ^{16}O, and ^{4}He beams impinging on two different targets of C and C_2H_4 will be employed, thus boosting fragments energy and making their detection possible. Fragmentation cross section on H target will be then obtained by subtraction of the C target from the C_2H_4 one [14]. However, the same configuration also allows measuring the projectile fragmentation of the mentioned beams exploiting direct kinematic. The design and optimization of the FOOT experimental setup was based on a simulation of 200MeV/u ^{16}O beam impinging on a C_2H_4 target performed by means of the FLUKA MC code [15, 16]. The results show that fragments with Z ⩾ 3are forward peaked and mainly confined in a 10° angle with respect to the primary beam direction, emitted with a kinetic energy per nucleon distribution centered around that of primary beam. Instead, light fragments are characterized by an extremely broad spectrum in terms of both angular and kinetic energy distribution. Moreover, FOOT requires a table-top experimental setup, easily movable and capable to perform measurements in different experimental and treatment rooms of several European facilities where the beams of interest are available. Following the mentioned constraints, FOOT includes two complementary experimental setup: an electronic setup based on a magnetic spectrometer to identify fragments heavier than helium, and a setup exploiting the emulsion chamber capabilities to detect the light charged fragments (Z ⩽ 4). The electronic setup (figure 1) consists in a pre-target monitor region, a magnetic spectrometer, a scintillator detector with ΔE and Time-Of-Flight (TOF) capabilities and a calorimeter. The detector measures momentum, energy release, TOF and kinetic energy of each produced fragment in the solid angle of the apparatus. The pre-target region monitors the beam direction providing the number of primary ions impinging on the target and their interaction point. It is composed of two elements: a thin plastic scintillator Start Counter(SC) detector, which provides the trigger to the whole experiment, the start time for the TOF

Figure 1. Schematic view of the FOOT electronic setup. The distance between the target and the ΔE-TOF scintillator varies depending on the energy of the primary beam. It is of ~1 m for a 200 MeV/u beam and ~3 m for a 700 MeV/u beam.

Figure 2. (Left) Schematic view of the emulsion spectrometer setup placed downstream the Start Counter and the Beam Monitor. (Right) Scheme of the emulsion spectrometer composition.

evaluation and the measurement of the incoming primary flux; a Beam Monitor (BM) drift chamber to measure the new beam direction after crossing the SC and impinging point of the primary beam on the target and discard deviated tracks produced by beam fragmentation in SC. A great precision on the beam direction is necessary to apply the inverse kinematic. The magnetic spectrometer provides production vertex and momentum of the fragments through the tracking outside the magnetic field. It includes two cylindrical permanent magnets (PM), four pixel sensors of Vertex (VTX) detector placed between target and PM, two additional planes of pixel sensor detectors (ITR) placed in between the two PM and three layer of Microstrip Silicon Detector (MSD) placed beyond the second magnet. The downstream region is composed of two orthogonal planes of plastic Scintillator bars (TW) and a 24 cm thick BGO calorimeter (CAL) to provide the stop signal for the TOF evaluation, the measurement of the fragments energy loss and kinetic energy. The distance of the TW and CAL with respect to the target position changes according to the primary beam energy: TW and BGO are placed at about 1 m from the target center-of-mass rest frame in the case of a primary beam energy of 200 MeV/u, while at 700 MeV/u their position is moved downstream to about 3 m in order to have the same angular acceptance. Alternatively, an Emulsion Spectrometer (ES) placed behind the SC and the BM (figure 2) was designed in order to measure low Z fragments produced outside the magnetic spectrometer acceptance. The ES for the FOOT experiment has been designed with passive materials alternated to nuclear emulsions films, making a first section dedicated to the interaction and vertexing, followed by a charge identification section and the last one devoted to the momentum measurements.

Table 1. Resolutions on TOF, ΔE, E_{kin} and p evaluated through dedicated beam tests or MC simulations by means of a standard Kalman tracking algorithm. The best performances always refer to the highest fragment charges.

$\sigma(TOF)$	[70–250] ps
$\sigma(p)/p$	[3–5]%
$\sigma(\Delta E)/\Delta E$	[3–10]%
$\sigma(E_{kin})/E_{kin}$	[1.5–2.5]%

Table 2. Reconstructed charge Z and number of mass A_{χ^2} evaluated through a χ^2 minimization method for fragments with $Z \leqslant 8$ generated by a 200 MeV/u and 700 MeV/u ^{16}O beam impinging on a 5 mm C_2H_4 target. The values and the associated errors are the mean value and the σ of the Gaussian fit of the distributions, respectively. The width in the distribution is due to the resolutions applied to the quantities involved in the charge and mass evaluation.

	200 MeV/u		700 MeV/u	
Fragment	**Z**	A_{χ^2}	**Z**	A_{χ^2}
^{1}H	1.0 ± 0.1	1.0 ± 0.1	0.9 ± 0.1	1.0 ± 0.1
^{4}He	2.0 ± 0.1	4.0 ± 0.2	2.0 ± 0.2	4.0 ± 0.2
^{7}Li	3.0 ± 0.1	7.1 ± 0.3	3.0 ± 0.2	7.0 ± 0.3
^{9}Be	4.1 ± 0.2	9.1 ± 0.4	4.0 ± 0.2	9.0 ± 0.4
^{11}B	5.1 ± 0.2	10.2 ± 0.4	5.0 ± 0.2	11.1 ± 0.4
^{12}C	6.1 ± 0.2	12.2 ± 0.5	6.0 ± 0.2	12.1 ± 0.5
^{14}N	7.1 ± 0.2	14.3 ± 0.6	7.0 ± 0.2	14.1 ± 0.6
^{16}O	8.2 ± 0.2	16.4 ± 0.7	8.0 ± 0.2	16.1 ± 0.6

A detailed description of all the detectors involved in the electronic setup, as well as the emulsion spectrometer can be found in [11].
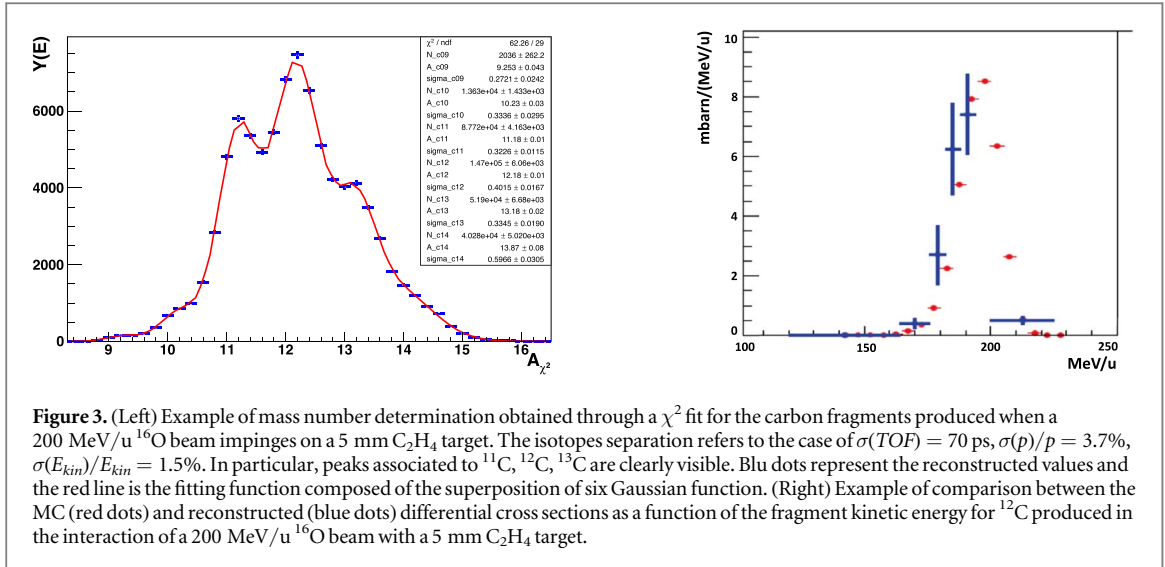
3. Fragments identification

The fundamental quantities to uniquely identify a fragment in terms of charge Z and mass number A are the Time-Of-Flight (TOF), momentum (p), energy loss (ΔE) and kinetic energy (E_{kin}). Therefore, only particles crossing all the apparatus can be correctly identified, in fact ΔE, E_{kin}, TOF, p are provided respectively by TW, CAL, SC and TW signals combination, the fragment charge evaluation coupled with the rigidity (p/Z) evaluated by the tracking and bending in the magnetic field. Several data taking for SC, TW and CAL detectors have been performed to experimentally evaluate the resolutions on TOF, ΔE and E_{kin}. The resolution on p has been estimated through MC simulations using a standard Kalman tracking algorithm. The performances are reported in table 1.

The study of fragment reconstruction capability of the FOOT experiment has been performed based on FLUKA simulations. The mentioned resolutions have been applied as a Gaussian smearing to the corresponding quantities produced by the simulation in order to obtain an experimental-like data sample. The fragment charge Z is measured by combining ΔE and TOF measurements in the Bethe-Block equation [17, 18]. Results reported in table 2 show that fragments charge reconstruction precision ranges between $\sim$6% for hydrogen to $\sim$2% for oxygen allowing a clear identification of the different charges. The redundancy of subdetectors in the FOOT electronic apparatus is the key factor for the isotopic discrimination. In fact, the fragment number of mass A evaluation can be achieved by combining TOF, p and E_{kin} measurements in three different equations, as follow:

$$A_1 = \frac{p}{U\gamma\beta c} \qquad A_2 = \frac{E_k}{(\gamma - 1)Uc^2} \qquad A_3 = \frac{p^2c^2 - E_k^2}{2Uc^2E_k} \tag{1}$$

where U is the Unified Atomic Mass ($\sim$931.5 MeV), β is the fragment velocity provided by the tracking path L coupled with the TOF measurement, defined as $\beta = L/(TOF \cdot c)$, and γ is the Lorentz factor. The three mass determinations are correlated by a common quantity for each couple of equations. The position of the peak for a fragment number of mass evaluated with the equations (1) are centered around the expected values, with a mass resolution of $\sim$3.5% for A_2 and slightly worst for A_1, while it is larger than 8% in the A_3 case due to the error

Figure 3. (Left) Example of mass number determination obtained through a χ^2 fit for the carbon fragments produced when a 200 MeV/u ^{16}O beam impinges on a 5 mm C_2H_4 target. The isotopes separation refers to the case of $\sigma(TOF) = 70$ ps, $\sigma(p)/p = 3.7\%$, $\sigma(E_{kin})/E_{kin} = 1.5\%$. In particular, peaks associated to ^{11}C, ^{12}C, ^{13}C are clearly visible. Blu dots represent the reconstructed values and the red line is the fitting function composed of the superposition of six Gaussian function. (Right) Example of comparison between the MC (red dots) and reconstructed (blue dots) differential cross sections as a function of the fragment kinetic energy for ^{12}C produced in the interaction of a 200 MeV/u ^{16}O beam with a 5 mm C_2H_4 target.

propagation. A standard χ^2 minimization approach performing a fit to the mass values is then pursued in order to get the best number of mass estimation among the three evaluation. A χ^2 cut can be additionally applied to discard the bad reconstructed fragments. In order to reduce only of ~20% the statistics of the heavier fragments ($Z \geqslant 3$), a $\chi^2 < 5$ cut has been selected by looking at the χ^2 distribution as a function of the mass number. Table 2 reports the mass number value and its resolution for some of the identified fragments. An example of mass number determination retrieved with a χ^2 minimization method is reported in figure 3(Left) for the carbon fragments generated in the interaction of a 200 MeV/u oxygen beam with a polyethylene target. The isotopes separation is clearly visible. A fit with a superposition of several Gaussian functions is applied, in order to evaluate each isotope yield, mass and relative resolution. The charge identification and the χ^2 minimization procedure assure a complete isotopic identification of each fragment generated in the beam-target interaction. In the case of 700 MeV/u primary beam, only A_1 provides a reliable number of mass estimation. In fact, the probability of secondary fragmentation and neutrons emission inside the CAL is particularly pronounced at higher energy, thus leading to a frequent underestimation of the fragment kinetic energy.

The production differential cross section of the fth fragment with respect to its emission angle θ or production kinetic energy E_{kin} is defined as follow:
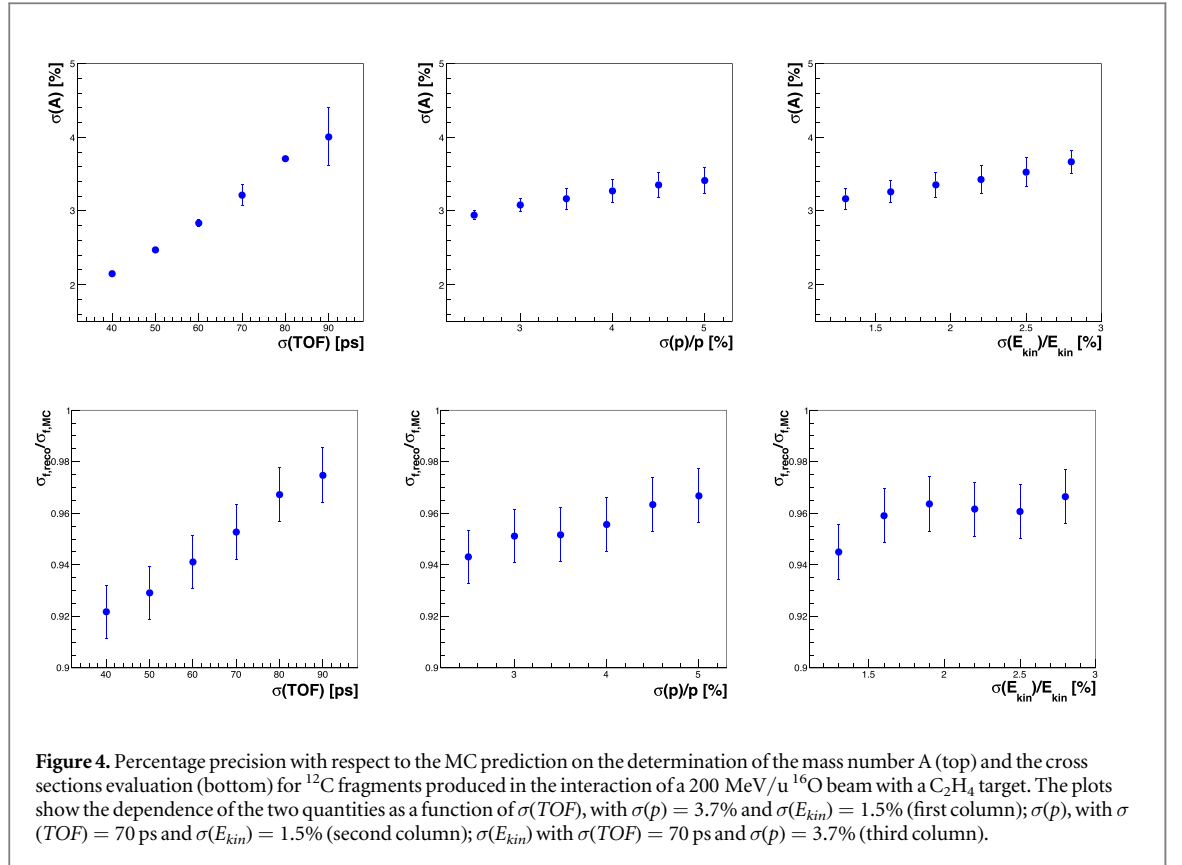
$$\frac{\sigma_f}{d\theta} = \frac{(Y_f(\theta) - Bgk_f)^U}{N_{prim}N_t\Omega_\theta\epsilon} \qquad \frac{\sigma_f}{dE_{kin}} = \frac{(Y_f(E_{kin}) - Bgk_f)^U}{N_{prim}N_t\Omega_E\epsilon} \tag{2}$$

where Y is the fragment yield, N_{prim} is the number of primary beam particles, N_t is the number of target scattering center, Ω_θ and $\Omega_{E\,kin}$ are the angular and energy phase spaces respectively, ϵ is the reconstruction efficiency. The *background* (*Bkg*) represents the misidentification probability of the charge and mass number of a fragment, while the *unfolding* (*U*) process corrects the fragments distribution of the experimental effects that can lead to a wrong counts of the produced fragments [19]. Figure 3(Right) reports an example of comparison between the true and reconstructed cross section evaluated for ^{12}C fragments produced with only MC events in the interaction of a 200 MeV/u ^{16}O beam impinging on a polyethylene target. The result with a 700 MeV/u primary beam is analogue. By integrating over the whole energy or angle range, the total cross section is retrieved. The procedure has been applied at data concerning both C_2H_4 and C targets, in order to evaluate the result on H by difference.

4. Performances study

A performances study varying the resolution on *TOF*, p and E_{kin} has been performed in order to understand which detectors mostly affect the precision on the mass number determination (referred to as $\sigma(A)$) and the cross sections evaluation with respect to the MC prediction (referred to as $\frac{\sigma_{f,reco}}{\sigma_{f,MC}}$). An example of the dependence of $\sigma(A)$ and $\frac{\sigma_{f,reco}}{\sigma_{f,MC}}$ from the *TOF*, p or E_{kin} resolutions evaluated by keeping the other two fixed at the standard precision (respectively 70 ps, 3.7% and 1.5%) is reported in figure 4 for ^{12}C fragments. The plots show that $\sigma(A)$ spans between 2.1% and 4.0%, while the reconstructed total cross section presents a general agreement with the MC value inside ~8%. The global underestimation of the latter should be related to an overestimation of the efficiency by a constant factor at present under investigation. In fact, the analysis

Figure 4. Percentage precision with respect to the MC prediction on the determination of the mass number A (top) and the cross sections evaluation (bottom) for ^{12}C fragments produced in the interaction of a 200 MeV/u ^{16}O beam with a C$_2$H$_4$ target. The plots show the dependence of the two quantities as a function of $\sigma(TOF)$, with $\sigma(p) = 3.7\%$ and $\sigma(E_{kin}) = 1.5\%$ (first column); $\sigma(p)$, with $\sigma(TOF) = 70$ ps and $\sigma(E_{kin}) = 1.5\%$ (second column); $\sigma(E_{kin})$ with $\sigma(TOF) = 70$ ps and $\sigma(p) = 3.7\%$ (third column).

underlines also a general overestimation of $\sim$7% of the number of events reconstructed with respect to MC prediction.

5. Real data analysis

Experimental data collected in April 2019 at the GSI Helmholtz Center for Heavy Ion Research (GSI) [20] with a 400MeV/u ^{16}O beam impinging on a 5 mm graphite target ($\rho = 1.83$ g cm^{-3}) have been analyzed to perform the first FOOT fragments charge separation based on real data. A total of $4.5 \cdot 10^4$ events were acquired with a partial FOOT electronic setup, composed of the pre-target region (SC and BM), VTX, TW and a module of CAL placed downstream the target at a distance of 2.23 m from SC. The energy release ΔE in the TW was previously calibrated with ^{16}O, ^{12}C and protons beams [21]. The charge Z of a particle impinging on the TW in position i is evaluated by inverting the Bethe-Bloch formula [17, 18], as follows:

$$Z_i = \sqrt{\frac{\Delta E_i}{\rho \delta x} \frac{\beta^2 A_S}{K Z_S} \left(\frac{1}{2} log \frac{2 m_e c^2 \beta^2 \gamma^2 W_{max}}{I^2} - \beta^2 \right)^{-1}} \qquad (3)$$

where $\beta = \dfrac{d}{c \cdot TOF_i}$, d is the distance traveled by the particle and δx is the thickness of the two TW layers ($\delta x = 6$ mm). TOF_i is evaluated by combining the start time provided by SC and the corresponding stop time obtained from TW. The plot reported in figure 5 shows that different charged fragments can be well discriminated and an estimation of the charge values and the corresponding uncertainties can be obtained by applying a Gaussian fit to each peak. The results are reported in table 3, together with the differences with respect to the expected charge value. The distribution does not contain any hydrogen particles because of the experimental threshold chosen in the SC signals to discriminate the electronic noise, which also cuts events below a certain charge. The results are satisfactory and in agreement with those predicted in the MC based study presented in section 3. However, the results can be considered as preliminary due to the very low statistics of events correctly reconstructed ($\sim 4.3 \cdot 10^3$ events) and will be further improved with higher statistics experimental campaign foreseen in 2021.
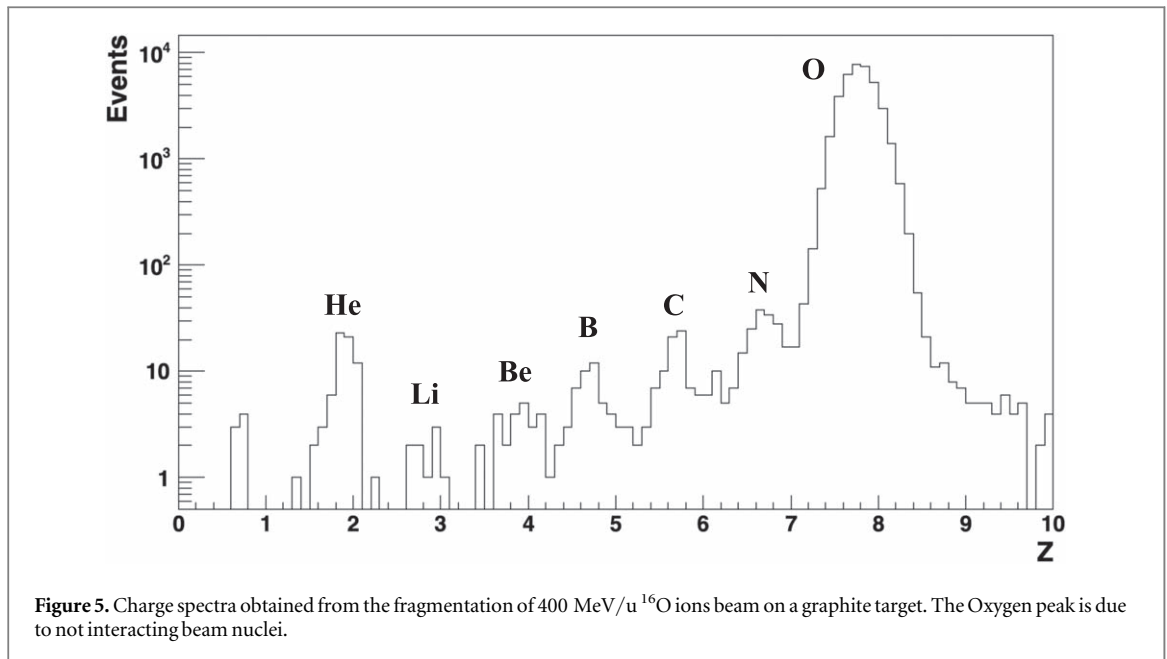
Figure 5. Charge spectra obtained from the fragmentation of 400 MeV/u ^{16}O ions beam on a graphite target. The Oxygen peak is due to not interacting beam nuclei.

Table 3. Preliminary charge evaluation obtained by applying Gaussian fits to the charge spectra of fragments produced in the interaction of a 400 MeV/u ^{16}O beam with a 5 mm graphite target. The charge values and the associated errors are the mean value and the σ of the Gaussian fits, respectively. The third column represents the difference between the reconstructed charge value and the expected one.

Particle	Z	Diff [%]
H	—	—
He	2.5 ± 0.1	25.5
Li	3.1 ± 0.2	1.9
Be	4.7 ± 0.2	15.3
B	5.6 ± 0.2	10.1
C	6.4 ± 0.2	6.7
N	7.3 ± 0.2	3.7
O	7.9 ± 0.2	−1.8

6. Discussion

The FOOT (FragmentatiOn Of Target) experiment has been designed to measure with a great accuracy nuclear fragmentation cross sections for beams (i.e. ^{16}O, ^{12}C, ^{4}He, p) and targets (i.e. O, C, H) relevant in particle therapy and space radioprotection. The investigation of the former requires primary beam energies up to 400 MeV/u, while the latter up to 800 MeV/u. The experiment has been originally conceived to study target fragmentation occurring in the interaction of a proton beam with matter. The process is particularly difficult to experimentally investigate, thus requiring a complex setup and fine experimental strategies, such as the inverse kinematic approach. However, the same apparatus can be exploit to investigate the projectile fragmentation process. By measuring and combining p, TOF, E_{kin} and ΔE, the FOOT setup is able to identify the produced fragments in terms of charge and mass, as well as their generation energy and production angle. In this work, a feasibility study based on FLUKA MC simulations is presented, as well as the charge separation analysis of the first real data sample collected by a partial electronic setup. The experimental resolutions of the detectors have been applied to the simulated sample in order to recreate experimental-like data. The present detectors performances (i.e. σ(TOF) $\simeq 70$ ps, $\sigma(p)/p \simeq 3.7\%$ and $\sigma(E_{kin})/E_{kin} \simeq 1.5\%$) allow to identify fragment charge with a precision spanning from ∼6% for hydrogen to ∼2% for oxygen and the fragment number of mass with a resolution ranging between ∼3.5% and ∼4.5%, both for particles identified at primary beam energies of 200 MeV/u and 700 MeV/u. A feasibility study of the differential cross sections with respect to the kinetic energy of each carbon isotope generated in the beam-target interaction have been evaluated with only MC data and afterwards

compared with the MC prediction. The results on C_2H_4 and C targets have been directly assessed, while differential cross sections on a H target is retrieved by combining through subtraction the results on the formers. For all the targets investigated, the results on the total cross section are compatible within the uncertainties with the MC predictions. A performances study varying the resolution on *TOF*, p and E_{kin} in a reasonable range around their experimental values has been performed in order to estimate the impact of each detector on the accuracy of the cross section determination. The results point out a dependence of the latter on the reconstructed kinematics quantities. Therefore, the highest precision is required for each subdetector in order to decrease the discrepancies with respect to MC prediction. In particular, the dependence on the *TOF* precision is much stronger than the influence of p and E_{kin} resolutions. The analysis of the first experimental data acquired with the FOOT apparatus in 2019 underlines a good capability of the setup to discriminate well the produced fragments charge.
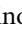
7. Conclusions

The FOOT experiment proposes several experimental campaigns to improve the characterization of the complex radiation field generated by the interaction of medium-high energy beams (200–1000 MeV/u) with targets for applications in particle therapy and space radiation protection. The fragments charge discrimination obtained from the analysis of the first experimental data collected in 2019 validates the precision predicted by the study of MC data. Hence, the findings of this work lay the foundation for future experimental measurements and analysis foreseen in 2021.

Data availability statement

The data generated and/or analysed during the current study are not publicly available for legal/ethical reasons but are available from the corresponding author on reasonable request.

ORCID iDs

S Colombi ⓘ https://orcid.org/0000-0002-5650-8941
N Bartosik ⓘ https://orcid.org/0000-0002-7196-2237
M Durante ⓘ https://orcid.org/0000-0002-4615-553X
R Hetzel ⓘ https://orcid.org/0000-0002-6142-6609
M Marafini ⓘ https://orcid.org/0000-0003-1282-0383
C Massimi ⓘ https://orcid.org/0000-0003-2499-5586
I Mattei ⓘ https://orcid.org/0000-0002-6819-1646
F Murtas ⓘ https://orcid.org/0000-0003-2587-273X
V Patera ⓘ https://orcid.org/0000-0003-1999-8424
F Pennazio ⓘ https://orcid.org/0000-0001-8323-0132
C Sanelli ⓘ https://orcid.org/0000-0003-1938-6102
E Scifoni ⓘ https://orcid.org/0000-0003-1851-5152
G Sportelli ⓘ https://orcid.org/0000-0001-9982-0292
F Tommasino ⓘ https://orcid.org/0000-0002-8684-9261

References

[1] Durante M and Loeffler J 2010 *Nat. Rev. Clin. Oncol.* **7** 37–43
[2] Durante M and Debus J 2018 *Semin. Radiat. Oncol.* **28** 160–7
[3] Golovkov M *et al* 1997 *Adv. Hadron Therapy Int. Congr. Ser.* **1144** 316
[4] Rovituso M *et al* 2017 *Phys. Med. Biol.* **62** 1310–26
[5] Marafini M *et al* 2017 *Phys. Med. Biol.* **62** 1291–309
[6] Zuofeng L 2009 *Int. J. Radiat. Oncol. Biol. Phys.* **73** 1602
[7] Tang J *et al* 1997 *Brit. J. Cancer* **76** 220–5
[8] Tommasino F and Durante M 2015 *Cancers* **7** 353–81
[9] Norbury J *et al* 2012 *Health Phys.* **103** 640–2
[10] Nelson G 2016 *Radiat. Res.* **185** 351–3
[11] Battistoni G *et al* 2021 *Front. Phys.* **8**
[12] Battistoni G *et al* 2017 *PoS* **BORMIO2017** 023
[13] Patera V *et al* 2017 *PoS* **INPC2016** 128
[14] Doudet J *et al* 2013 *Phys. Rev. C* **88** 024606
[15] Böhlen T *et al* 2014 *Nucl. Data Sheets* **120** 211

[16] Battistoni G *et al* 2016 *Front. Oncol.* **6** 116
[17] Bethe H 1930 *Ann. Phys.* **397** 325–400
[18] Bloch F 1933 *Z. Physik* **81** 363–76
[19] D'Agostini G 1995 *Nucl. Instrum. Meth.* A **362** 487–98
[20] Eickhoff H *et al* 1999 *Strahlenther Onkol.* **175** 21–4
[21] Kraan A *et al* 2021 *Nucl. Instrum. Meth.* **1001** 165206 A